

13 Transitions from order to chaos

This lecture is mainly based on the books *From simple models to complex systems* by M. Cencini et al. and *Chaos In Dynamical Systems* by E. Ott, and on Chapter 10 in Stogatz.

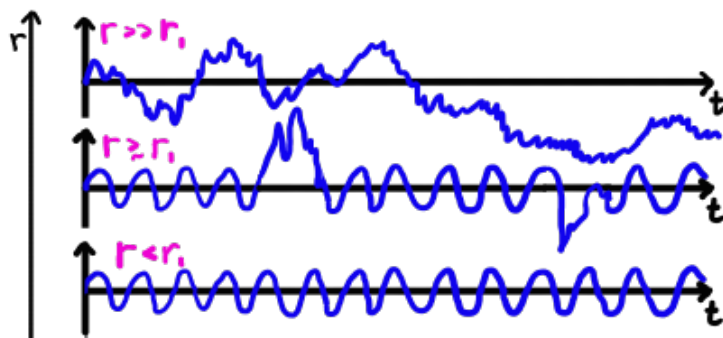
There are several ways in which regular dynamics (stable fixed points or periodic/quasiperiodic motion) transforms into chaos as some system parameter r is changed. The transition is very different in dissipative systems and in Hamiltonian systems.

13.1 Transition to chaos in dissipative systems

In numerical simulations and in experiments it is observed that the transition from regular motion to chaos in dissipative systems always pass through a strange attractor of low fractal dimension, before potential attractors of higher fractal dimension are reached. Below a few mechanisms for the transition from regular dynamics to strange attractors of low dimension are summarized.

13.1.1 Intermittency transition (Pomeau-Manneville)

Fixed point or periodic orbit becomes unstable at a single bifurcation r_1 , leading to chaos characterized by intermittency.



Intermittency Nearly regular motion interrupted by occasional short irregular outbursts at irregular time intervals. As control parameter is increased, the bursts become more and more frequent until system becomes fully chaotic.

Explanation Just after the bifurcation ($r > r_1$ but $r \approx r_1$) the system has bottlenecks where the dynamics is regular (ghost of fixed point, or weakly unstable periodic orbit or fixed point). After leaving a bottleneck the dynamics becomes irregular (intermittent outburst) until a new bottleneck is reached.

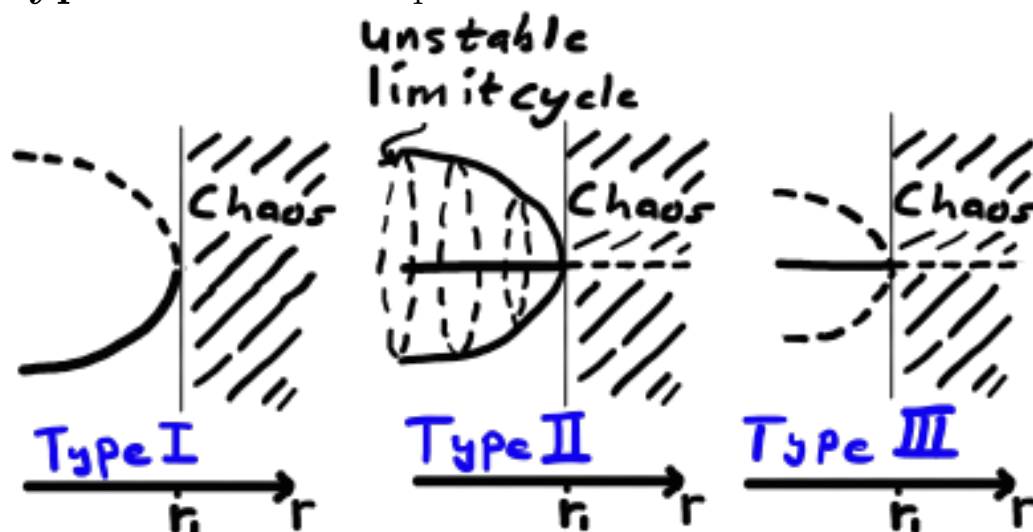
This often occurs in systems with saddle-node bifurcations between cycles: as the stable periodic orbit disappears in a saddle-node bifurcation a bottleneck is formed due to the slow dynamics close to the former limit cycle. In these systems the average time of regular motion is of order $1/\sqrt{r}$ (the time to pass the ghost of a saddle-node, see Lecture 2).

The intermittency bifurcation is classified in three types depending on how the stable attractor becomes unstable:

Type I Saddle-node bifurcation

Type II Subcritical Hopf bifurcation (stable fixed point and unstable periodic orbit merge into an unstable spiral)

Type III Subcritical pitchfork bifurcation



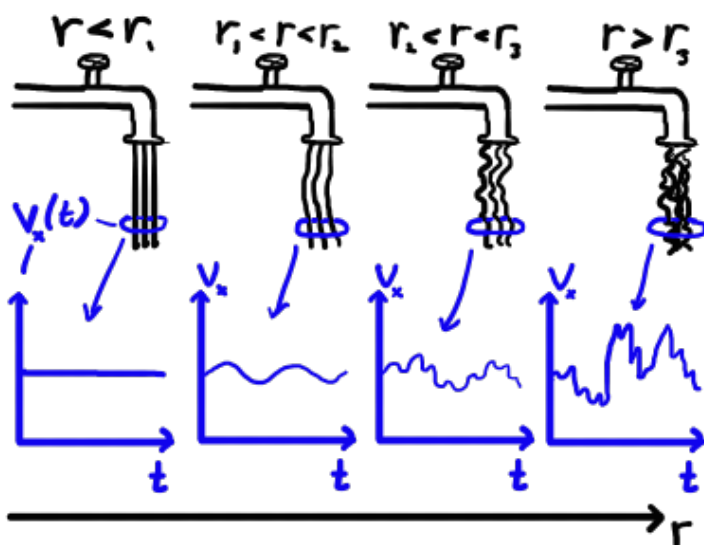
The intermittency transition can for example be found in Lorentz equations and some examples where it is found experimentally are in fluid flows, BZ-reaction, and driven non-linear semiconductors.

13.1.2 Ruelle-Takens

Typical example Transition from laminar to turbulent flow as the Reynolds number r (dimensionless flow speed) is increased, for exam-

ple the water stream from a faucet flows regularly at small flow speeds and irregular (turbulent) for larger speeds.

Transition to chaos by a sequence of three bifurcations r_1, r_2, r_3 :



r_1 : Fixed point (constant flow velocity) to limit cycle with single frequency (supercritical Hopf bifurcation)

r_2 : The limit cycle obtains two frequencies (periodic|quasiperiodic)

r_3 : Chaos with strange attractor (Ruelle-Takens showed that periodic orbits with three frequencies are structurally unstable, i.e. extremely unlikely to be observed in real-world systems)

The Ruelle-Takens transition are experimentally found in various fluid systems.

13.1.3 Period-doubling bifurcation (Feigenbaum)

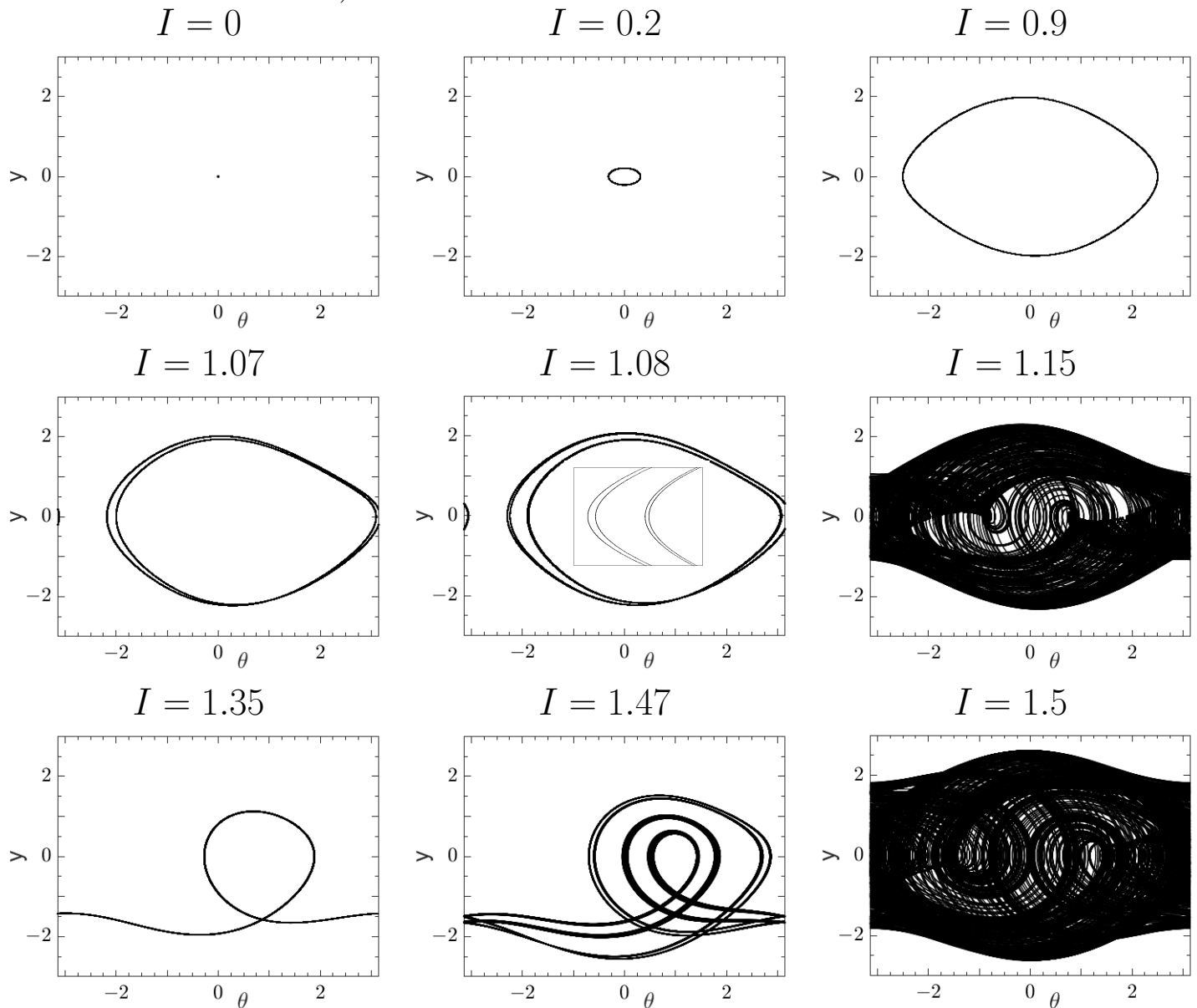
Example: Periodically driven pendulum Consider a pendulum with a periodic torque in dimensionless units (c.f. Lecture 9)

$$\ddot{\theta} = - \underbrace{\alpha \dot{\theta}}_{\text{damping}} - \underbrace{\sin \theta}_{\text{gravity}} + \underbrace{I \cos(\omega_F t)}_{\text{periodic forcing, angular frequency } \omega_F}$$

Write as an autonomous dynamical system with $y = \dot{\theta}$ and $\tau = t$

$$\begin{aligned} \dot{\theta} &= y \\ \dot{y} &= -\alpha y - \sin \theta + I \cos(\omega_F \tau) \\ \dot{\tau} &= 1 \end{aligned}$$

Trajectories with $\alpha = 1/2$, $\omega_F = 2/3$ (period time $T_F = 2\pi/\omega_F$) for some values of I projected on the θ - y plane for large times (neglecting an initial transient):



Note that the dynamics is three-dimensional:

- Trajectories are allowed to cross in the projection.
- Stable, periodic trajectories in the projection are not limit cycles in the three-dimensional dynamics (the time coordinate is not periodic).

Upon changing I , keeping α and ω_F fixed, we observe the following:

- When $I = 0$ trajectories are attracted to the stable fixed point at $\theta = y = 0$.
- When $I = 0.2$, linearisation theory applies and the system can be solved analytically: For large times the solution takes the form $\theta(t) = A(\omega_F) \cos(\omega_F t + \phi(\omega_F))$, i.e. the pendulum oscillates with the frequency of the applied forcing. The amplitude A and phase shift ϕ depend on the applied frequency ω_F and the eigenfrequency ω_0 (imaginary part of the eigenvalue at $\theta = y = 0$ when $I = 0$) of the pendulum. Period time T_F .
- When $I = 0.9$ oscillations are larger and the linearized theory no longer applies. Period time T_F .
- When $I = 1.07$ a period-doubling bifurcation has occurred and the pendulum oscillates with double period time $2T_F$.
- When $I = 1.08$ another period-doubling bifurcation has occurred (see inset for zoom-in), pendulum oscillates with quadruple period time $4T_F$.
- As I increases to around $I = 1.15$ period-doubling bifurcations happens at closer and closer values of the bifurcation parameter I . Eventually, the period becomes infinitely long at a finite bifurcation value (close to $I = 1.15$). The projected trajectory has an infinite period, i.e. it is aperiodic and the motion is chaotic. If we let $t \rightarrow \infty$ the projection plot would become uniformly black within the reachable part of phase space.
- When $I = 1.35$ a stable window appears. Period time T_F .
- When $I = 1.45$ period-doubling bifurcation in the stable window. Period time $2T_F$.
- When $I = 1.47$ period-doubling bifurcation in the stable window. Period time $4T_F$.
- When $I = 1.5$ close to chaotic again

The behavior observed for the driven pendulum outlines a general period-doubling transition to chaos of periodic orbits (to have a period-doubling requires $d > 2$, otherwise trajectories cross).

The period-doubling cascade consists of an infinite sequence of bifurcations $r_1, r_2, \dots, r_\infty$ where period time doubles. Assume the system has a periodic orbit in the form of a loop for $r < r_1$.

At $r = r_1$ this bifurcates to a double loop (periodic orbit of period 2).

At $r = r_2$ the periodic orbit bifurcates to a periodic orbit of period 4.

At subsequent, increasingly denser values of r_i , the periodic orbit bifurcates into periodic orbits of growing period 2^i .

Finally, as $r \rightarrow r_\infty$ (r_∞ can be finite because bifurcation values r_i becomes denser with increasing i) the dynamics becomes aperiodic (chaotic).

For values of r larger than r_∞ the system typically exhibit chaos with ‘windows’ of periodic motion (c.f. the behaviour of the driven pendulum with $I > 1.15$ and $I \approx 1.35$).

The period-doubling bifurcation has been observed experimentally in for example lasers, plasmas, BZ reaction, and in fluid dynamics.

Universality It is possible to show that for certain subclasses of systems (systems that can be projected on a unimodal one-dimensional map) the period-doubling is universal. For example, for r_i with large i the difference between bifurcations shrinks with a constant factor (Feigenbaum constant)

$$\delta = \lim_{n \rightarrow \infty} \frac{r_n - r_{n-1}}{r_{n+1} - r_n} = 4.669 \dots$$

This is a constant of nature, it is independent of the form of the system.

This universality is easier to discuss in one-dimensional maps, and is discussed further in Computational Biology 1.

13.2 Transition to chaos in Hamiltonian systems

Hamiltonian systems were introduced in Lecture 5: Newtons law $\mathbf{F} = m\ddot{\mathbf{x}}$ without friction written on dynamical-system form:

$$\begin{aligned}\dot{\mathbf{x}} &= \frac{\partial H}{\partial \mathbf{p}} \\ \dot{\mathbf{p}} &= -\frac{\partial H}{\partial \mathbf{x}}.\end{aligned}\tag{1}$$

with position \mathbf{x} , momentum $\mathbf{p} = m\dot{\mathbf{x}}$, and energy function

$$H(\mathbf{x}, \mathbf{p}) = \underbrace{\frac{|\mathbf{p}|^2}{2m}}_{\text{kinetic energy}} + \underbrace{V(\mathbf{x})}_{\text{potential energy}}.$$

In Lecture 5 it was shown that Hamiltonian systems (1) are volume conserving, $\nabla \cdot \mathbf{f} = 0$, and that energy $E = H(\mathbf{x}, \mathbf{p})$ is conserved.

The Hamiltonian flow can be written more compactly

$$\dot{\boldsymbol{\xi}} = \mathbb{S} \frac{\partial H}{\partial \boldsymbol{\xi}} \equiv \mathbf{f},\tag{2}$$

with

$$\boldsymbol{\xi} \equiv (\mathbf{x}, \mathbf{p}), \quad \mathbb{S} \equiv \begin{pmatrix} \mathbb{O}_{N \times N} & \mathbb{I}_{N \times N} \\ -\mathbb{I}_{N \times N} & \mathbb{O}_{N \times N} \end{pmatrix},$$

where \mathbb{S} is a ‘symplectic matrix’.

13.2.1 Integrable systems

Since no attractors can exist in volume-conserving systems, trajectories are either periodic|quasiperiodic (integrable systems) or aperiodic (non-integrable, chaotic systems). The periodic|quasiperiodic motion in integrable systems becomes apparent in ‘action-angle coordinates’.

13.2.2 Action-angle coordinates

Consider the case of one spatial dimension $H(x, p)$. Bounded trajectories are periodic orbits (isolines of constant energy). Make a canonical (preserves the form in Eq. (2), and thus area conservation) change of coordinates to ‘action’ variable I

$$I = \frac{1}{2\pi} \oint dx p$$

and a so far unspecified angle variable ϕ . The integral runs over a periodic orbit. Energy conservation $H(x, p) = E \Rightarrow p$ can be rewritten in terms of x and $E \Rightarrow I$ depends on E only. Consequently $I(t) = I(0) = \text{const.}$

Another consequence: Since $I = f(E)$ we have $H = E = f^{-1}(I)$, i.e. H is a function of I only (not ϕ) in the new coordinates.

To preserve the form Eq. (2) we have (these equations define ϕ)

$$\begin{aligned} \dot{\phi} &= \frac{\partial H(I)}{\partial I} \equiv \omega(I) \\ \dot{I} &= -\frac{\partial H(I)}{\partial \phi} = 0 \end{aligned}$$

with solution $I(t) = I(0)$ and $\phi(t) = \phi(0) + \omega(I(0))t$.

I selects a periodic trajectory with angular frequency ω . Angle variables ϕ are useful for finding frequencies of rotations or librations without solving the equations of motion.

Example: Harmonic oscillator Hamiltonian $H(x, p) = p^2/(2m) + m\omega_0^2 x^2/2 = E$. This is an equation for elliptic orbits with axes of magnitude $\sqrt{2mE}$ and $\sqrt{2E/(m\omega_0^2)}$. The action coordinate becomes

$$\begin{aligned} I &= \frac{1}{2\pi} \oint_C dx p \quad \left[\text{Green's theorem: } \oint_C (Ldx + Mdp) = \int \int_S \left(\frac{\partial M}{\partial x} - \frac{\partial L}{\partial p} \right) dx dp \right] \\ &= -\frac{1}{2\pi} \int \int_S dx dp \quad \left[\text{Harmonic oscillator has clockwise } C \Rightarrow \text{sign}(S) = -1 \right] \\ &= \frac{\text{Area of ellipse}}{2\pi} = \frac{1}{2} \sqrt{2mE} \sqrt{\frac{2E}{m\omega_0^2}} = \frac{E}{\omega_0}. \end{aligned}$$

I is a function of E only as expected. It follows that $H = E = \omega_0 I$ and $\dot{\phi} = H'(I) = \omega_0$ is the angular frequency.

Higher dimension Hamiltonian systems in one spatial dimension are examples of integrable systems. The dynamics can be solved formally for all times in terms of I and ϕ (while the integral in I is not always possible to evaluate explicitly).

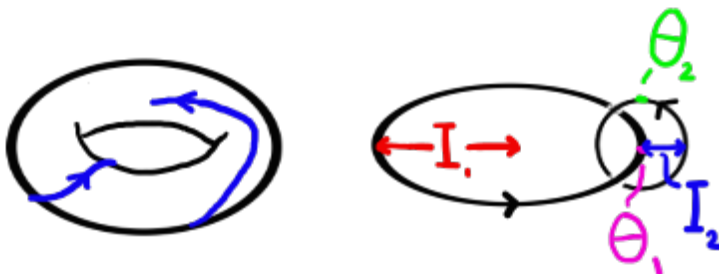
The notion of integrability is generalised to higher dimensions d if there exists d constants of motion $C(\mathbf{x}, \mathbf{p})$ such that

$$\begin{aligned}\dot{C} &= \dot{\mathbf{x}} \frac{\partial C}{\partial \mathbf{x}} + \dot{\mathbf{p}} \frac{\partial C}{\partial \mathbf{p}} \\ &= \frac{\partial H}{\partial \mathbf{p}} \frac{\partial C}{\partial \mathbf{x}} - \frac{\partial H}{\partial \mathbf{x}} \frac{\partial C}{\partial \mathbf{p}} \equiv \{C, H\} = 0.\end{aligned}$$

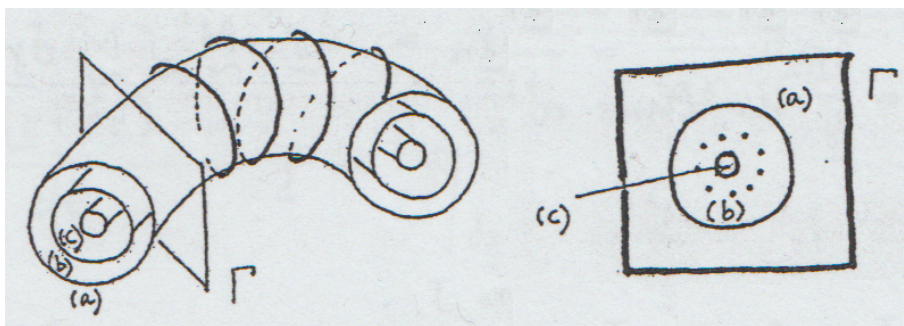
If the Hamiltonian system has d independent constants of motion (such as energy, momentum in each coordinate, angular momentum etc.) it is integrable. Solutions are constrained to a d -dimensional hypersurface defined by $C_i(\mathbf{x}, \mathbf{p}) = \text{const.}$, $i = 1, \dots, d$. The solutions are d -dimensional non-intersecting tori. In terms of action-angle coordinates, the equations of motion are

$$\begin{aligned}\dot{\phi} &= \frac{\partial H(\mathbf{I})}{\partial \mathbf{I}} \equiv \boldsymbol{\omega}(\mathbf{I}) = \text{constant vector} \\ \dot{\mathbf{I}} &= \mathbf{0}.\end{aligned}$$

When $d = 2$ the dynamics of the angle variables is identical to that of uncoupled oscillators on a torus (discussed in Lecture 9).



Using the constant action variables I_i as the torus radii, non-intersecting solutions for all initial conditions can be visualized:



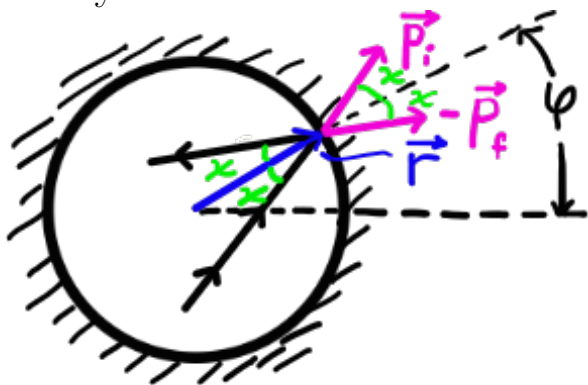
The motion show periodicity or quasiperiodicity depending on whether the ratio $\omega_1(\mathbf{I})/\omega_2(\mathbf{I})$ is rational or not, i.e. if there exists integers k and l such that $k\omega_1 + l\omega_2 = 0$, then trajectories close into periodic orbits. In the illustration above, trajectory (b) is periodic (rational torus) and trajectories (a) and (c) are quasiperiodic (irrational torus).

13.2.3 Perturbation of a system that remains integrable

In few exceptional cases the dynamics of an integrable Hamiltonian system remains integrable after a small perturbation.

Example: Circular billiards Consider a circular billiard (dimensionality $n = 4$, i.e. two spatial dimensions). As we discussed in Lecture 9, this is an example of an integrable system because it has two constants of motion: energy $E = p^2/(2m)$ and angular momentum with respect to the circle center.

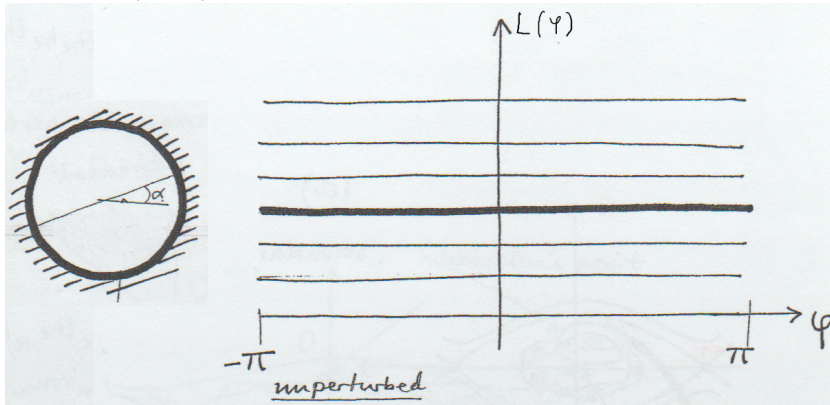
Conservation of angular momentum The angular momentum w.r.t. the center is: $L = |\mathbf{r}||\mathbf{p}| \sin \alpha$, where α is the angle between \mathbf{r} and \mathbf{p} . For the circular billiard, the reflection angle χ is the same for any collision.



Before the collision with the boundary, the angle between \mathbf{r} and \mathbf{p}_i

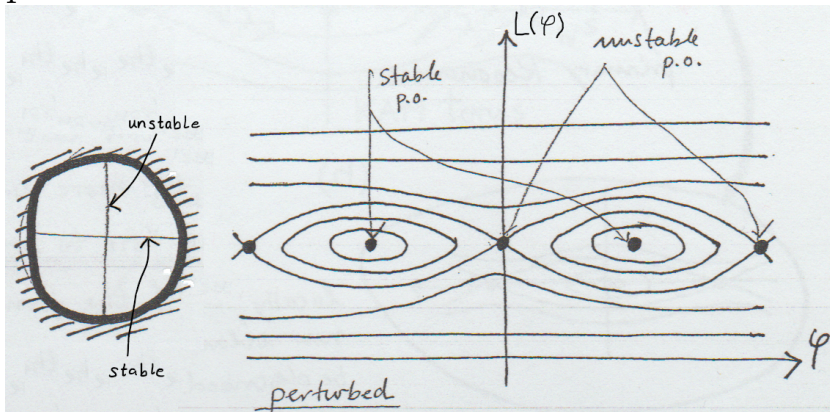
equals the reflection angle, $\alpha = \chi$, and after the collision the angle between \mathbf{r} and \mathbf{p}_f are related by $\alpha = \pi - \chi$. Since $\sin \chi = \sin(\pi - \chi)$ the angular momentum is conserved at collisions. In addition, uniform motion has constant angular momentum and angular momentum is therefore a conserved quantity.

One example of a periodic orbit in the circular billiard is shown below (left):



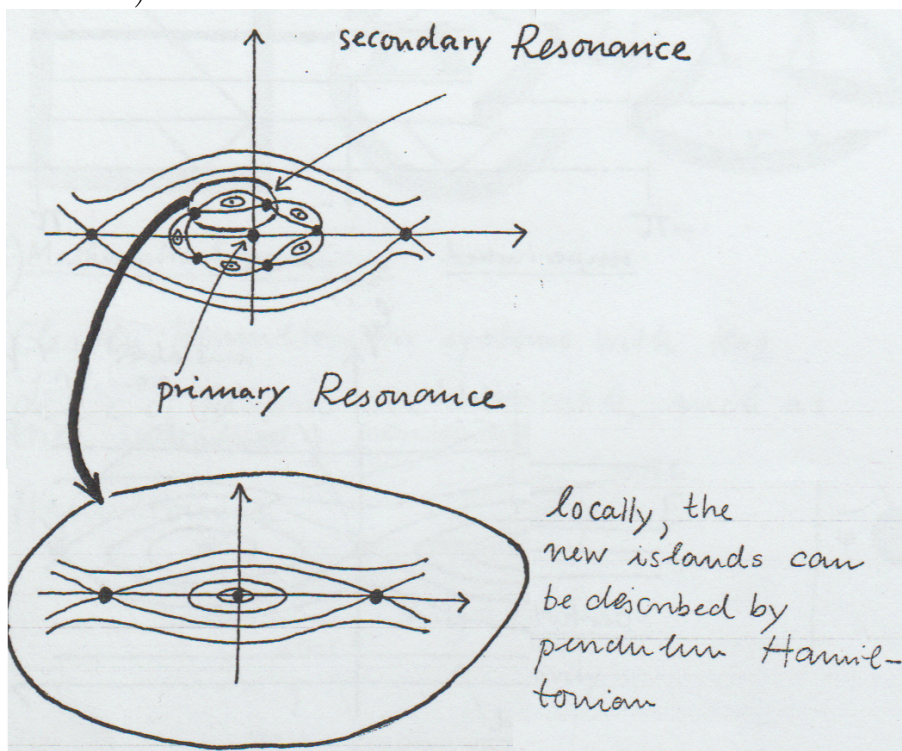
To visualize the dynamics, it is convenient to sample the angle φ and angular momentum $L(\varphi)$ at collisions, neglecting the intermediate motion. To the right, the dynamics is illustrated by plotting φ and $L(\varphi)$ upon collisions with the boundary. Thin lines show irrational tori and the thick line shows the rational tori corresponding to the periodic motion in the left panel (for each initial condition α we obtain a discrete set of two points, averaging over initial conditions we obtain the continuous line). Due to circular symmetry, there is a continuous family of periodic orbits, determined by parameter α (left).

After a small perturbation as shown below (left), only two isolated periodic orbits remain:



Thus, a small perturbation breaks up the rational torus into one (marginally) stable (small perturbations do not grow) and one unstable (small perturbations grow) periodic orbit. Mathematically, the system in the vicinity of the new fixed points can be described by the Hamiltonian of an ideal pendulum. The system is integrable because there exists two sets of constants of motion, one inside the separatrices (heteroclinic orbits between saddle points) and one outside. This follows from the fact that the stable and unstable manifolds of the saddle points join smoothly. As we shall see in the next section, this is not the generic case,

If the system is perturbed slightly more, other rational tori break up, possibly one of those created around the new stable periodic orbit. In the latter case a chain of integrable islands (which locally look like phase-space pictures of the pendulum) is created (secondary resonance):



Under stronger perturbations, higher-order resonances appear, creating a hierarchy of island chains (nested tori).

Two important observations

1. **KAM theorem** Tori with rational ω_1/ω_2 breaks up first. Tori with strongly irrational ω_1/ω_2 break up last (KAM tori). Any real quotient ω_1/ω_2 can be approximated by a continued fraction

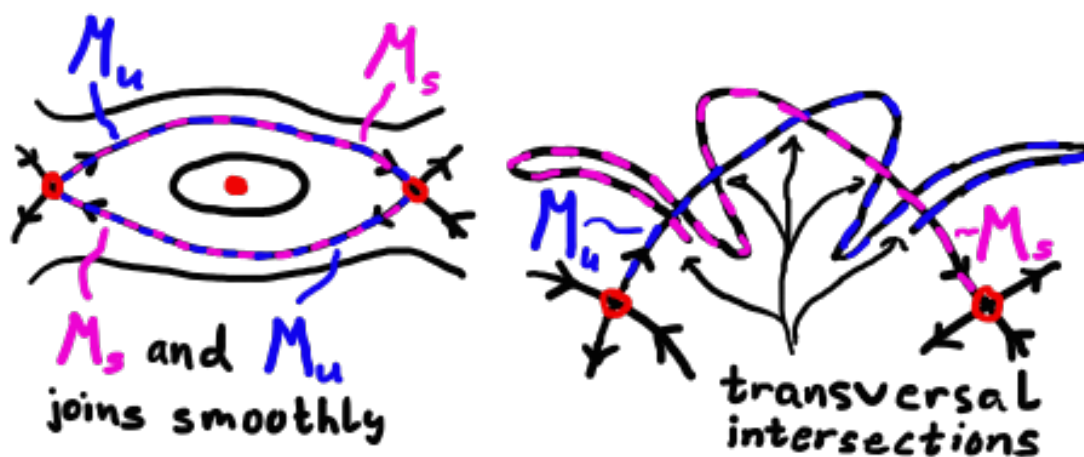
$$\frac{\omega_1}{\omega_2} = a_1 + \frac{1}{a_2 + \frac{1}{a_3 + \frac{1}{a_4 + \dots}}}$$

with a sequence a_n with $n = 1, 2, \dots$. The continued fraction converge quicker the faster the coefficients in the sequence a_n grow. Strongly irrational ω_1/ω_2 have sequences a_n that grow slowly. The limiting case of a non-growing (constant) sequence a_n with $a_n = 1$ for all n gives the golden ratio $G = (\sqrt{5} + 1)/2$. Tori with $\omega_1/\omega_2 = G \pm k$ with k an integer are the last ones to break up (KAM tori).

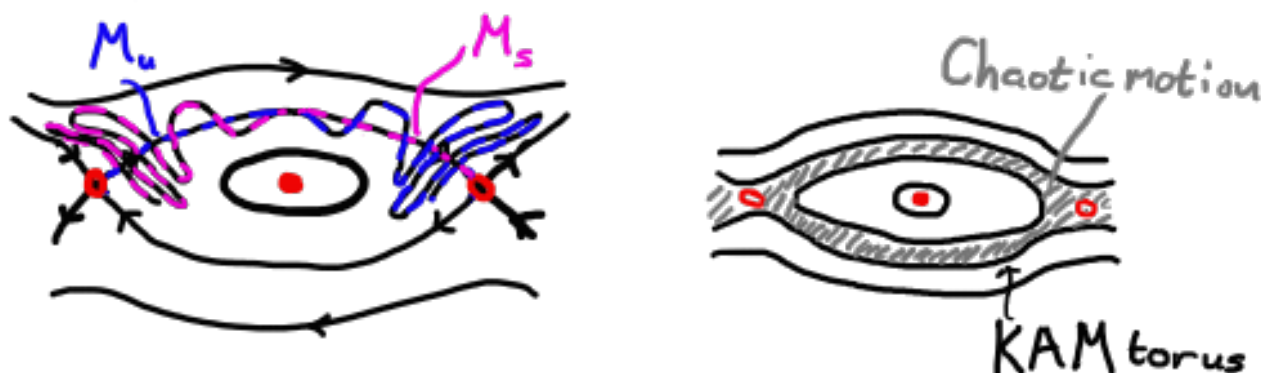
2. **Poincaré-Birchoff theorem** When a torus of rational ω_1/ω_2 breaks up, an equal number of (marginally) stable and unstable fixed points appear. Around the (marginally) stable fixed points, new resonant tori are formed that generates a new sequence of (marginally) stable and unstable fixed points appear. Iterating gives a self-similar structure of fixed points around each (marginally) stable fixed point (regular islands).

13.2.4 Transition to chaos

In the example for the circular billiard above, chains of integrable islands are generated when rational tori break up. Locally the dynamics can be described by the Hamiltonian of a pendulum. This is a special case, more generally integrability is destroyed by small perturbations of Hamiltonian systems. Typically the manifolds of the newly created unstable fixed points do not join smoothly in heteroclinic trajectories as for the circular billiard (left), but rather intersect transversally (right):



Note that the plotted dynamics is projected (e.g. by plotting one component of position and momentum at regular time intervals), allowing the manifolds to cross. It is possible to show that, under quite general conditions, the manifolds of the projected dynamics will intersect an infinite number of times if they intersect once, similar to the right panel above. This means that the manifolds become more and more intricate closer to the saddle and a thin band of chaotic motion is formed:



The band is bounded by KAM tori that are more resistant to perturbations. If the perturbation is increased, an infinite hierarchy of bands of chaotic motion is created (similar to the hierarchy of islands for the circular billiard). When perturbation is strong enough also KAM tori break up and global chaotic motion is obtained (close inspection on small scales often reveals tiny integrable islands).

The transition to chaos outlined above is valid in two spatial dimensions. In higher dimensions the chaotic regions are no longer sandwiched between remaining KAM tori, allowing chaotic trajectories of slightly perturbed systems to wander off in phase space (Arnold diffusion).